Characterization of complex networks by higher order neighborhood properties

Roberto F. S. Andrade, José G. V. Miranda, Suani T. R. Pinho

Instituto de Física - Universidade Federal da Bahia

40.130-240 - Salvador - Brazil

and Thierry Petit Lobão

Instituto de Matemática - Universidade Federal da Bahia,

40210-340 - Salvador - Brazil

(Dated: February 6, 2008)

Abstract

A concept of higher order neighborhood in complex networks, introduced previously (PRE **73**, 046101, (2006)), is systematically explored to investigate larger scale structures in complex networks. The basic idea is to consider each higher order neighborhood as a network in itself, represented by a corresponding adjacency matrix. Usual network indices are then used to evaluate the properties of each neighborhood. Results for a large number of typical networks are presented and discussed. Further, the information from all neighborhoods is condensed in a single neighborhood matrix, which can be explored for visualizing the neighborhood structure. On the basis of such representation, a distance is introduced to compare, in a quantitative way, how far apart networks are in the space of neighborhood matrices. The distance depends both on the network topology and the adopted node numbering. Given a pair of networks, a Monte Carlo algorithm is developed to find the best numbering for one of them, holding fixed the numbering of the second network, obtaining a projection of the first one onto the pattern of the other. The minimal value found for the distance reflects differences in the neighborhood structures of the two networks that arise from distinct topologies. Examples are worked out allowing for a quantitative comparison for distances among a set of distinct networks.

PACS numbers: 89.75.Hc, 89.75.Fb, 89.20.Hh, 02.10.Ox

I. INTRODUCTION

In recent years, complex networks have become one of the major research themes in complex systems. They allow for an interesting interplay between mathematics and physics through the well-established theories of graphs [1] and statistical mechanics. Despite the fact that they are simply defined in terms of sets of N nodes and L links connecting pairs of nodes, they can exhibit a very complex structure. In this way, they have attracted the attention of scientists, from most different areas, aiming to investigate their potential usefulness in the description of geometrical and dynamical properties of complex systems [2, 3, 4].

The huge development in this research area comes along with the proposition of parameters that capture some essential properties that such objects may have. Most of the current works in the literature expresses the quantitative results in terms of a hand full of indices or quantifiers [5, 6, 7], like the average number of links per node $\langle k \rangle$, clustering coefficient C, mean minimal distance among the nodes $\langle d \rangle$, diameter D, and the assortativity degree A. Also of relevance are certain relations that express how these quantifiers are composed, like $p(k)$, the probability distribution of nodes with k links, the distribution of each individual node clustering coefficients $C(k)$ with respect to its node degree, and the average degree of the neighbors of a node with k links $\langle k_{nn}(k) \rangle$.

The quoted set of indices have been used as they can be easily evaluated, and have a very clear intuitive geometrical and topological meaning. Despite their ability in characterizing these most relevant features of networks, other parameters can be proposed to account for other properties that are overlooked by the above quoted set. The actual relevance of the information brought by a new parameter depends whether it is, in a certain sense, *orthogonal* to the set of parameters that had been used so far. In such case, its evaluation contributes either to emphasize similarities among a set of networks, or to uncover differences among them. Therefore, new parameters may indeed become relevant to identify differences between networks that could have been thought to be similar in a more restricted space of characterization parameters.

From our point of view, it is important to probe the network with respect not only to the immediate, close neighborhood of a node, but also how all pairs of nodes are related among themselves, from the nearest up to the maximal distance D. This leads to the concept of

higher order neighborhoods, providing a clearer picture on the intermediate and large scale structures of the network. It is worth mentioning that other authors [8, 9, 10, 11] also defend similar positions to ours, having proposed several strategies to investigate network properties that advance beyond the immediate vicinity of a node. However, as it shall be clear in the sequel, our approach is quite different from those just presented in the related literature.

In a previous work [12], we have indicated how to obtain all higher order neighborhoods of a node in a network R with the help of Boolean product of matrices. According to the definition introduced there, two nodes in R are neighbors of order $O(\ell), \ell = 1, 2, ..., D$, when the shortest path connecting them, along links in R, has ℓ steps. Each $O(\ell)$ neighborhood of R determines a network $R(\ell)$, just by connecting pairs of nodes that are ℓ steps apart in R. Each $R(\ell)$ is fully described by the corresponding adjacency matrix $M(\ell)$. This process has three main consequences: i) it unfolds, in a straightforward way, a large amount of information contained in the adjacency matrix M of R; ii) doing this, it puts the information at hand for the analysis of the higher order neighborhood properties; iii) it offers, quite naturally, to condense all information extracted from M in a single neighborhood matrix $\widehat{\mathbf{M}}$, defined in terms of the set $\{M(\ell)\}$, which can be used for a much complete characterization of R than M. To attest the consistency and usefulness of the proposed framework, that work also presented a characterization of the $O(\ell)$ neighborhoods by means of the eigenvalue spectra of the higher order adjacency matrices $M(\ell)$, for several types of networks.

The current work has two main purposes, both of which are related to developments of the quoted procedure and, to our opinion, they contribute to provide a more complete insight into the properties of the analyzed networks. The first one is to characterize the larger structure properties by the analysis of all $O(\ell)$ neighborhoods of R. Like in the analysis of the spectral density, the method amounts to analyze all networks $R(\ell)$, taking into account their representation through the corresponding $M(\ell)$. As they are *bona fide* networks, their immediate neighborhood can be analyzed with the same set of indices used to characterize R, i.e., $\langle k(\ell)\rangle$, $C(\ell)$, $p(k;\ell)$, $A(\ell)$, and the distribution $C(k;\ell)$. The exact values of the global network parameters D and $\langle d\rangle$ are readily obtained after the decomposition process. In addition to that, the adopted procedure provides, as by-product, the necessary measures to evaluate the fractal dimension d_F of a network, according to the scheme [13] proposed recently.

In regard to the second series of results, we first use the matrices $\widehat{\mathbf{M}}$ for the purpose of visualizing the large scale structure of the networks. Afterwards, they are systematically explored to define and evaluate a measure of the distance between two networks with the same number of nodes. This implementation provides a still more direct comparison between networks than that obtained by the comparison of a larger number of indices as discussed above. Such procedure would not be so efficient if defined only on the basis of the original adjacency matrix M, as it requires the information on the complete neighborhood structure present in $\widehat{\mathbf{M}}$.

The rest of this work is so organized: in Section II we briefly review the main steps required to describe the higher order networks, and discuss how the quantities obtained in this process can be used to describe and represent other properties of networks. In Section III we discuss the behavior of $C(\ell)$, $\langle k(\ell)\rangle$, $p(k;\ell)$, $C(k;\ell)$, $A(\ell)$, and d_F for a large number of networks. We consider the small-world (SW) [14] and scale-free (SF), generated according, respectively, to the Newman [5] and the Barabasi-Albert [15] algorithms, the Erdös-Renyi (ER) [16], the Cayley tree (CT), the Apollonian network (AN) [17]. We also include in this list two well known structures, the Diamond Hierarchical Lattice (DHL) and the Wheatstone Hierarchical Lattice (WHL), which have been largely used in the context of spin models in statistical mechanics [18]. A comparison of the values for $C(\ell)$ with similar parameters proposed in other works to characterize the topology of more distant neighbors is included [5, 8, 11]. In Section IV, we first show how a graphical color representation of the distinct neighborhoods can be worked out. This issue is followed by a discussion on the effect of node numbering in the network representation: we propose two renumbering procedures and a measure to estimate the distance, based on the neighborhood structure, between two networks with the same number of nodes. Results to this investigation are presented in Section V, for a subset of networks used in Section III. Finally, in Section VI, we close the work with final remarks and conclusions.

II. EVALUATING $O(\ell)$ NEIGHBORHOODS

The $O(\ell)$ neighborhoods can be easily evaluated if we represent a network R by its adjacency matrix M. The networks $R(\ell)$, defined in the Introduction, are expressed by the corresponding adjacency matrix $M(\ell)$. So, if $O_i(\ell)$ is the set of ℓ-neighbors of node i, we

obtain

$$M(\ell)_{ij} = \begin{cases} \delta_{\ell,\ell'}, & \text{if } j \in O_i(\ell') \\ 0, & \text{otherwise} \end{cases} \tag{1}$$

We note that $M = M(1)$ and, if we consider that each node belongs to $O(0)$ of itself, then $M(0) = I$, where I represents the identity matrix. As shown in [12], all $M(\ell)$ can be successively evaluated with the help of Boolean operations [20], using one single recurrence equation:

$$M(\ell) = (\bigoplus_{g=0}^{\ell-1} M(g)) \otimes M(1) - (\bigoplus_{g=0}^{\ell-1} M(g)). \tag{2}$$

The evaluation of all $M(\ell)$'s opens the path for a direct evaluation of many network parameters. Many of them are neighborhood dependent and, as far as we know, have not been considered before. On the other hand, the evaluation of some global parameters, which have usually been performed along other methods, can be obtained within this framework in a straight forward way. Let us first note that, once N is finite, for some large enough ℓ_{max} we find $M(\ell) \equiv 0, \forall \ell > \ell_{max}$, so that $D \equiv \ell_{max}$. Next, the knowledge of all $M(\ell)$ allows for the definition of the matrix $\widehat{\mathbf{M}}$, which carries all information on the shortest path between any two vertices i and j along the network. As, according to (1), $M(\ell)_{ij} = 1$ for only one ℓ, the definition

$$\widehat{\mathbf{M}} = \sum_{g=0}^{D} gM(g), \tag{3}$$

implies that, for all pairs $(i,j) \in O(\ell)$, $\widehat{\mathbf{M}}_{ij} = \ell$. Using color or gray code plots, the network neighborhood structure entailed in $\widehat{\mathbf{M}}$ can be visualized. The matrix $\widehat{\mathbf{M}}$ is only a bit differently defined from the so called *distance matrix* [21] used in the graph theory; it is reduced to that one in the case of a connected network. With the help of (3), the average minimal path for a node i is easily expressed by $d_i = (\sum_{j=1}^{N} \widehat{\mathbf{M}}_{i,j})/(N-1)$, leading, immediately, to the average $\langle d \rangle$.

Despite the fact that several complex networks have an intrinsic length scale, represented e.g., by $\langle d \rangle$ or D, there have been some attempts to associate fractal dimensions to these objects. The definition for a fractal dimension d_F, cited in the introduction, is deeply related to the concept of $O(\ell)$ neighborhoods. Indeed, once length is measured in R by the number of steps between nodes, scaling arguments lead to $L(\ell) \sim \ell^{d_F}$, where $L(\ell)$ counts the number of pairs of nodes that are ℓ steps apart. Within the current approach we obtain, at once, $L(\ell) = \sum_{i,j=1}^{N} M(\ell)_{i,j}/2$.

The evaluation of large scale structures in the network proceeds by considering each $R(\ell)$, represented by $M(\ell)$, as an independent network. Therefore, the parameters $C(\ell)$, $\langle k(\ell)\rangle$, $p(k;\ell)$, $C(k;\ell)$ and $A(\ell)$, which describe the local information on each $R(\ell)$, also provide information on the large scale structures of R. For any value of ℓ and node i, the node degree $k_i(\ell) = \sum_{j=1}^{N} M(\ell)_{i,j}$ and the node clustering coefficient $C_i(\ell) = \sum_{m\in O_i(\ell)} \sum_{j=1}^{N} M(\ell)_{i,j} M(\ell)_{m,j}/2$ are directly expressed in terms of elements of $M(\ell)$, while the other three quantities follow immediately by counting the number of occurrences of nodes with degree $k(\ell)$.

To characterize a data set represented as a network, one has to know whether all points are indeed connected among themselves in a single component, or partitioned into disjoint sub-networks. This important large scale property can be exactly answered provided the set $M(\ell)$ is evaluated. If the network consists of a single component, the quantity Z, defined by

$$Z \equiv \sum_{\ell=1}^{D} \sum_{j=1}^{N} M(\ell)_{i,j}, \tag{4}$$

always assumes the value $N(N-1)$. If $Z < N(N-1)$, two or more components are present and, in this case, their number and corresponding sizes can be evaluated as follows. First evaluate $\kappa_i = 1 + \sum_{\ell=1}^{D} k_i(\ell) < N-1, \forall i$. It counts the number of nodes in the specific component the node i belongs to, but it also indicates possible sizes for any other component. The maximal number of distinct values assumed by κ_i is limited by $(-1 + (1+8N)^{1/2})/2$. If $\sigma(\kappa)$ represents the number of nodes that share the same value of κ, the number of components of this size is simply $\sigma(\kappa)/\kappa$, what completes the characterization on the partition of the network. The adjacency matrix of a non connected network, by a suitable rearrangement of its nodes, may be reduced to a form of non-zero diagonal blocks, i.e. a direct sum of matrices of smaller order, each block corresponding to a connected component of the network. Because of this, one may just deal with connected networks, as we shall consider herein. We would like to emphasize that, for the sake of simplicity, we will restrict ourselves to present results only for undirected networks, without self links, and parallel links between any two nodes.

III. NEIGHBORHOOD CHARACTERIZATION

In this Section we present a characterization of $O(\ell)$ neighborhood for some standard networks. A flavor of this procedure is available in a previous work [12], where we concentrated on the spectral properties of the networks $R(\ell)$.

We have obtained a large amount of information on the neighborhood structure of networks. A summary of our most interesting results are depicted in Figures 1-6, where we draw the parameters quoted in the previous Section as function of the neighborhood ℓ. As anticipated in the Introduction, for the sake of a clearer discussion of our results, we use the methodology to investigate both geometrically grown networks (CT, AN, DHL, WHL), as well as many examples of well known networks, generated by precisely defined algorithms based on random generators, like ER, SF and SW networks. We discuss results for networks ranging from $N \sim 100$ up to a maximum of $N = 10000$ nodes, the choice of N depending on which aspect must be emphasized. As will be exemplified for some specific situations, our results remain quite independent of the size of the network, provided we scale properly the linking probabilities with N for those networks generated by random algorithms.

A. Clustering coefficient

Figure 1 shows how $C(\ell)$ behaves for the distinct networks. For the CT, $C(\ell)$ oscillates between zero and finite values for odd and even values of ℓ. This is explained by the fact that, as ℓ grows, the $R(\ell)$ networks assume, alternately, the structures of loop-less trees and Husimi cactuses, which entail a lot of triangles. This network has relatively large diameter, so that this behavior is sustained for several periods. Finite size effects cause a small decrease of the value of $C(\ell)$, what is enhanced when ℓ approaches D. Similar behavior is observed in many other situations, as the regular hyper-cubic lattices of dimension larger than 1, where triangles appear only for even ℓ's. It is also present in hierarchical structures as DHL. On the other hand, WHL behaves differently only for $\ell = 1$, when $C(1) = 0.57$, due to the presence of triangles. However they are absent for all larger order odd $\ell > 1$, so that an oscillatory pattern between 0 and non-zero values of $C(\ell)$ sets in.

A second common pattern for $C(\ell)$ is that of curve with a well defined maximum, taking finite values only over a finite range. It is found for SF networks generated according to

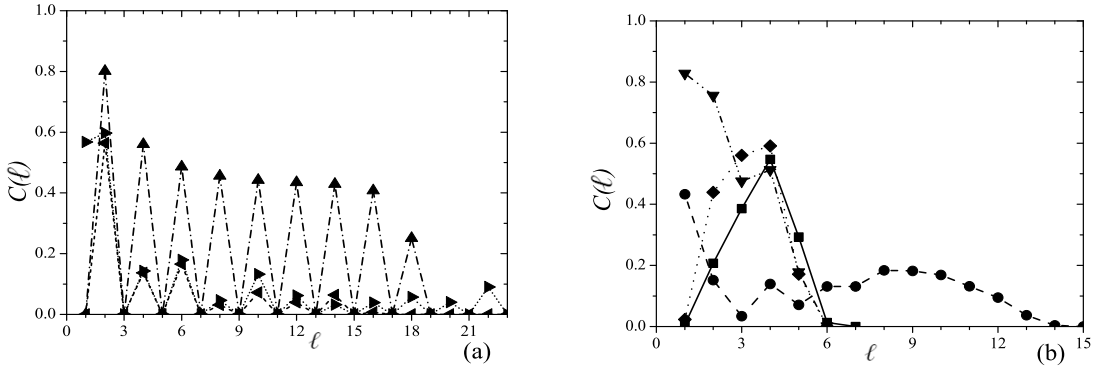

FIG. 1: Dependence of $C(\ell) \times \ell$ for the seven distinct networks. Conventions for (symbol, line) introduced here and used in the rest of this work are as follows: CT (up triangle, dash dot); AN (down triangle, dash dot dot); DHL (left triangle, short dash); WHL (right triangle, short dot); SF (diamond, dash); ER (square, solid); SW (circle, dash). The data were obtained for following values of N: (a) 1534 (CT), 684 (DHL), 1564 (WHL). (b) 3283 (AN), 2000 (SF); for ER, N=1000 and $p_a = 0.008$; for SW, $N = 1000, p_r = 0.2$.

the standard procedure [15], as well as for ER networks when, for instance, $N = 1000$ and connection probability $p = 0.008$. For the SF networks, this patterns emerges because neither the dominant hubs nor the nodes with lower k are likely to be connected in cliques. However, the hubs induce many lower k's nodes to form cliques at second and third order neighborhoods, explaining the sharp increase in the value of $C(\ell)$. The decrease in the value of $C(\ell)$ as $\ell \to D$ reflects the fact that the most part of all pairs of nodes have already been considered. For ER networks, similar arguments apply.

A third kind of pattern has also been observed for networks that are characterized by a large value of $C(1)$ as, e.g., the AN and SW networks. In the first case we start from a large value of $C(1) = 0.828$, following an almost monotonic decrease of $C(\ell)$. The same is observed for relatively large values of the rewiring probability p_r in SW networks.

We find important to notice, however, that if the behavior for the deterministic networks remain essentially the same as N grows, the same is not observed for SW and ER if we keep N constant and decrease the values for, respectively, p_r and the linking probability p_a. For both situations, oscillatory pattern between non-zero values emerges, indicating a similar

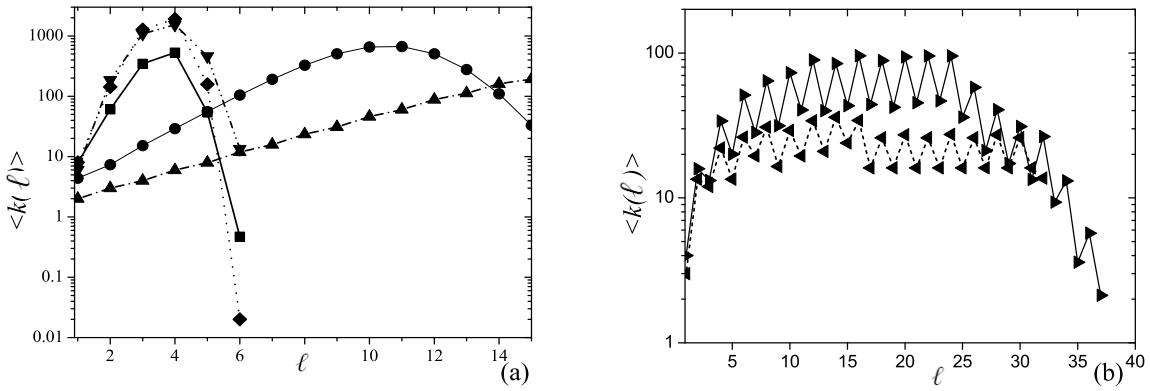

FIG. 2: Dependence of $\langle k(\ell)\rangle \times \ell$ for distinct networks. Symbols and lines follow the same convention as in Figure 1. (a) Values of N are the same used in Figure 1 for CT, AN, SF and ER, with $p_a = 0.008$. For SW, $N = 3500$ and $p_r = 0.2$. (b) Same values of N as in Figure 1 for DHL and WHL.

picture to those of geometrically constructed networks.

It is worth mentioning that other authors also proposed some generalized extensions of the notion of the clustering coefficient. In [8], it is investigated the issue if two neighbors of a given node are far from each other with a chosen distance x. Differently, in [9], the author asks if two nodes, at a chosen distance y of a given node, are neighbors of each other. There are also more ways to interpret the concept of neighborhood of a given node [11]. However, as far as we are aware, our approach, using the notion of neighbors of higher order, goes in different direction from that of the known literature.

B. Average degree

For regular lattices, the higher order neighbors of a site are roughly located on the surface of a hyper-sphere. Their number, which is equivalent to $\langle k(\ell)\rangle$, grows as ℓ^{dim-1}, where dim denotes the Euclidian dimension of the lattice. For the extreme situation of an exact CT, where the number of sites on the surface is of the same order of magnitude as those in the bulk, corresponding to $dim \to \infty$. This is reflected by an exponential increase of $\langle k(\ell)\rangle$ with ℓ, as shown in Figure 2a.

A similar behavior is expected to be found for many other complex networks, which have

a very small diameter. In Figure 2 we illustrate the behavior of $\langle k(\ell)\rangle$ for the same set of networks, showing that exponential increase is present for the majority of them. However, as the network is finite, $\langle k(\ell)\rangle$ must decrease for sufficiently large value of ℓ, making it difficult to assign a precise behavior for the dependence between $\langle k(\ell)\rangle$ and ℓ for these networks. In Figure 2a we find deviations from the exponential increase already when $\ell = 4$ for some networks. The DHL and WHL (Figure 2b) show a different pattern, consisting of an oscillating period 2 behavior, which is caused mainly by the contribution of the nodes introduced in the last hierarchy. For instance, in the DHL, these nodes are connected only to two other nodes but, for $\ell = 2$ and 3, they can have up to 9 and 4 neighbors. This situation is repeated for larger values of ℓ and also for the WHL.

C. Node distribution probability

The node distribution $p(k;\ell = 1)$ usually displays a bell shaped form for many kinds of networks found in nature, as well as those generated by the ER (Figure 3a) and SW (not shown) algorithms. Social and natural SF networks, the features of which we reproduce by the preferential attachment growth algorithm, are representative of another possible pattern, characterized by $p(k;1) \sim k^{-\gamma}$. For the purpose of a clearer picture, there we draw $\underline{P}(k;\ell) = \frac{1}{k}\int_k^\infty p(k';\ell)dk'$ for the usual SF, reproducing the value $\gamma \simeq 3$, as shown in Figure 3b for $\ell = 1$. In our investigations, we also find similar behavior for the AN, DHL and WHL networks, as shown in the points for $p(k)$ in the inset of this figure. The CT is a trivial case where $p(k;1)$ reduces to a single point.

For $\ell > 1$, our results show that the bell shaped pattern for $p(k;\ell)$ is reproduced when $\ell > 1$ for the ER and SW networks (see Figure 3a). As shown before, the average node degree increases with ℓ, so that it is natural that the curves for $p(k;\ell)$ are shifted towards larger values of k. The situation changes only for sufficient large $\ell \simeq D$, when finite size effects become relevant. Then, the majority of nodes have already reached their most distant neighbors while others miss only few connections. In this situation, the few non zero contributions to $p(k;\ell \simeq D)$ come for values of $k \sim 1$, so that the peak of the curve is shifted to the region close to the origin, as shown, in Figure 3a, for $\ell = 5$.

For the SF networks, the regions where the higher order $p(k;\ell)$'s receive significant contributions are also pushed to large values of $k(\ell)$. In general, the distributions loose the

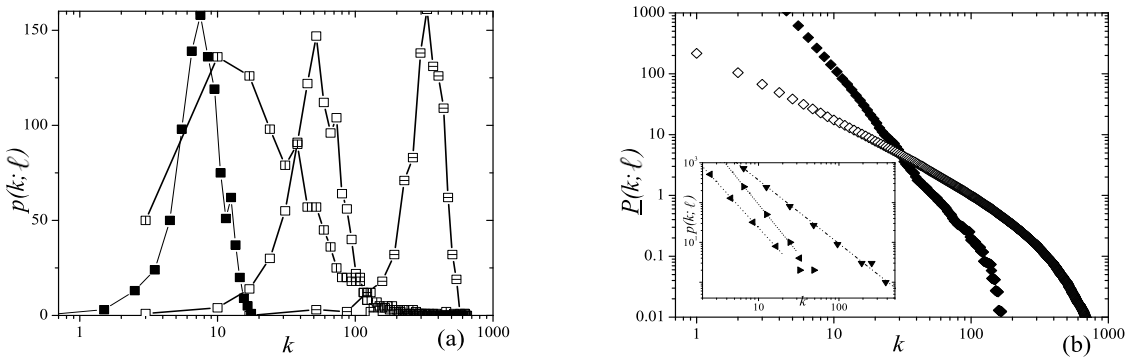

FIG. 3: Dependence of the probability distribution $p(k;\ell)$ and cumulative probability distribution $\underline{P}(k;\ell) \times k$ for distinct networks. (a) Curves for ER with same values of N and p_a used in Figures 1 and 2, when $\ell = 1$ (solid), 2 (hollow), 3 (horizontal dash) and 5 (vertical dash) squares. (b) In the large panel, $\underline{P}(k;\ell)$ follows power law for SF (when $\ell = 1$ (solid) and $\ell = 5 = D - 1$ (hollow)); in the inset, points indicate power law decay for $p(k;\ell = 1)$ in AN, DHL and WHL.

power law behavior, assuming distinct forms as ℓ increases. Exceptions are provided, e.g., in the example shown for the cumulative distribution $\underline{P}(k;\ell)$ in the large panel of Figure 3b. There we find a very interesting return to a power law distribution in the region of low values of k when $\ell = D-1$, with an exponent $\gamma \simeq 1.2$. To conclude this analysis, we remark that both DHL and WHL fail to display any noticeable alignment of points in any of their higher order neighborhood.

D. Hierarchical property

There are several distinct concepts of hierarchical organization, some of them stemming from the network framework, others from geometrical constructions, self similar fractal sets, etc. In this work, apart from using the word "hierarchical" to denote DHL and WHL, we refer to the concept introduced in [19], according to which a network has the hierarchical property if $C_i(1)$, the clustering coefficient of an individual node i, when are drawn as function of the individual node degree $k_i(1)$, shows a power law decrease. Much as observed with the analysis of the node distribution $p(k;\ell)$, evidences of hierarchical character for

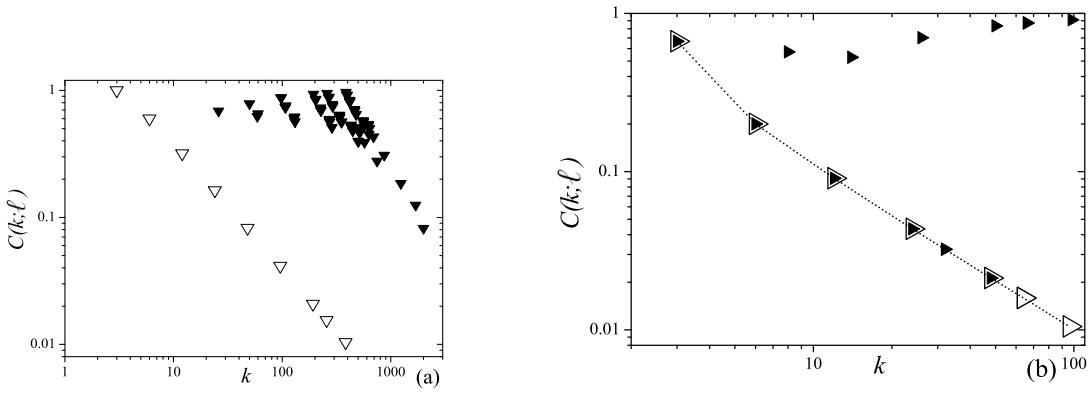

FIG. 4: Data for $C(k;\ell) \times k$ indicating hierarchical arrangement of nodes for AN (a) and WHL (b), respectively with $N = 3283$ and 7814 nodes. Data are drawn for $\ell = 1$ (hollow) and $\ell = 2$ (solid).

$R(\ell > 1)$, networks are rare, and are only found when $R(1)$ has already such character.

For the distinct networks we work with, indications of power law behavior for $\ell \geq 1$ are found for the AN and WHL networks, as illustrated in Figure 4a and 4b. Both networks show $C(k;1) \sim k^{-1}$ asymptotic dependence. On the other hand, DHL does not show this property since, as discussed before, $c_i(\ell = 1) \equiv 0, \forall i$.

We find slight evidences, for $\ell > 1$, of power law dependence in some subsets of points. In the particular case $\ell = 2$, for the AN, several points are aligned, seemingly building short patches that obey power law decrease. This very peculiar distribution of points is recurrent for all values of N that correspond to a full generation of the construction of AN.

For WHL, several points of the curves for $C(k;1)$ and $C(k;2)$ coincide exactly, so that a subset of points of $C(k;2) \times k$ still follows a power law decay. This is exemplary shown in Figure 4b, for the 7-th generation (7814 nodes). To explain the presence of this coincident points, we must take into account that, on increasing the generation of WHL, we add points to the region of large values of k of the $C(k;1)$ curve, while conserving all but one point of the previous generation. In Figure 4b, two newly added points, $k = 64$ and 96, are absent in the curve for the 6-th generation. They correspond to nodes with very large degree, e.g. at the root sites or the intermediate position, where the main bridge connecting two branches is placed. Now, when we look for pairs of second neighbors of the 7-th generation, we find

that part of them coincides exactly with first neighbors in the 6-th generation, so that the $C(k;2) \times k$ curve of the 7-th generation, for this subset, falls on the top the $C(k;1)$ curve of the 6-th generation. The other subset, which contributes to points that fall off the straight line, is formed by pairs of second neighbors that do not correspond to any first neighbors of the previous generation. For larger values of ℓ, we should still observe this truncated pattern only for the even values of ℓ. Indeed, as already discussed before, $C(\ell) = 0$ for odd ℓ's.

E. Assortativity degree coefficient

Several assortativity properties can be assigned to a network [2]. Each of them is quantified by a corresponding coefficient A, which indicates whether the pairs of nodes directly connected by a link are more likely to behave alike ($A > 0$) or dislike ($A < 0$). The assortativity degree coefficient [7], which takes into account the average degree of the nearest neighbors of a node of degree k represented by $k_{nn}(k)$, probes the degrees of the nodes at each side of a link. Here, we denote by $A(\ell)$ the coefficients that quantify the degree assortativity for the corresponding neighborhoods $O(\ell)$. Each $A(\ell)$ measures whether pairs of nodes, that are ℓ steps apart, are likely to be ℓ-connected to other nodes that have the same ℓ degree $k(\ell)$.

The results in Figure 5a-b display several kinds of patterns, indicating that the behavior of $A(\ell) \times \ell$ is very sensitive to the type of network. Figure 5a shows that SW networks have usual positive assortativity $A(\ell = 1) \simeq 0.2$. This value results from the contribution of the large majority of sites that are connected to their original neighbors in an ordered structure. On increasing ℓ, $A(\ell)$ remains positive for a large ℓ interval. After this phase, $A(\ell)$ goes through a steep descent to negative values, where it remains until $\ell = D$. This change reveals that the large ℓ neighborhoods completely loose the local character and nodes are overwhelmingly ℓ-connected to nodes with distinct ℓ-degree.

The results for a finite CT, in the same panel, are strongly biased by surface effects. In an infinite tree, all nodes have the same degree, so that $A(\ell = 1) = 1$. However, for any finite tree, a dissortative character is observed, which can be explained as follows: (i) The number of sites added in the last generation has the same order of magnitude of the existing sites; (ii) All of them have a distinct number of neighbors as those added before, the same happening to the nodes that are connected to them. In the evaluation of $A(1)$,

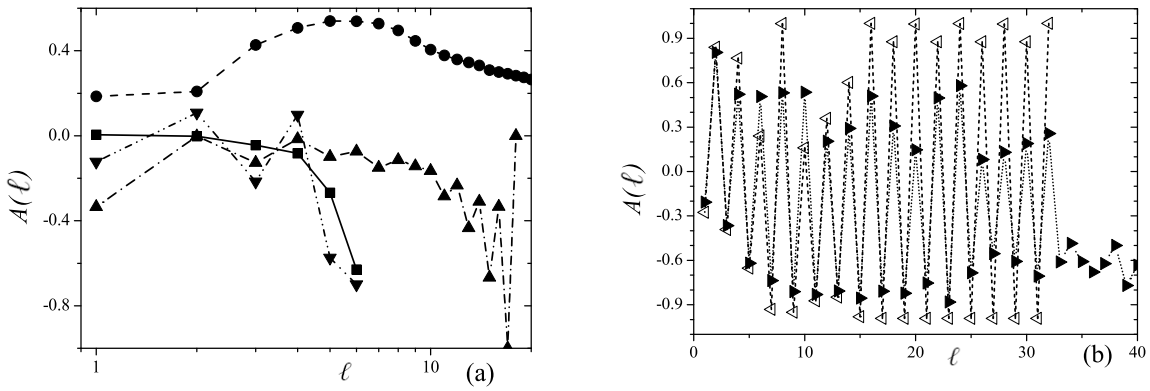

FIG. 5: Dependence of the degree assortativity coefficient $A(\ell)$ with ℓ. (a) Examples of assortative behavior for SW network, with $N = 3500$ and $p_r = 0.2$; neutral behavior for ER, with same parameter values as in Figure 1; oscillatory character for AN (N=3283); dissortative behavior for CT (N=1534). (b) Results for DHL and WHL with the same values of N as in Figure 1, indicate $\ell = 2$ periodic oscillations from dissortative to assortative behavior .

nodes with distinct degree on the end of all newly introduced links, contribute negatively, so that these contributions lead to a dissortative character to CT. The same occurs for larger values of ℓ, so that all $A(\ell)$ deviate strongly from the constant value 1 that they assume in an infinite tree. However, the constant value 1 can be recovered, in a finite sized network, if one neglects, successively, the effect of the ℓ-th lately added nodes.

For the ER networks, also illustrated in Figure 5a, pure randomness shows neutral behavior, hence $A(1) = 0$. Numerical simulations reproduce this result, which should be valid for several values of ℓ. However, for large ℓ, finite size effects end up by driving $A(\ell)$ to the negative region.

With respect to geometrically grown networks, oscillations between dissortative to assortative character is a common feature for AN, DHL and WHL. In the first situation (Figure 5a), the amplitude of variation of $A(\ell)$ is not so large and, due to the very small value of D, short lived. On the other hand, for DHL we have very large variations limited only by the extremal values ± 1 (see Figure 5b). This very peculiar behavior may be explained by noting that, for $\ell = 1$, no node has neighbors with the same degree as itself. On the other hand, when $\ell = 2$, the number of nodes with second order neighbors having the same

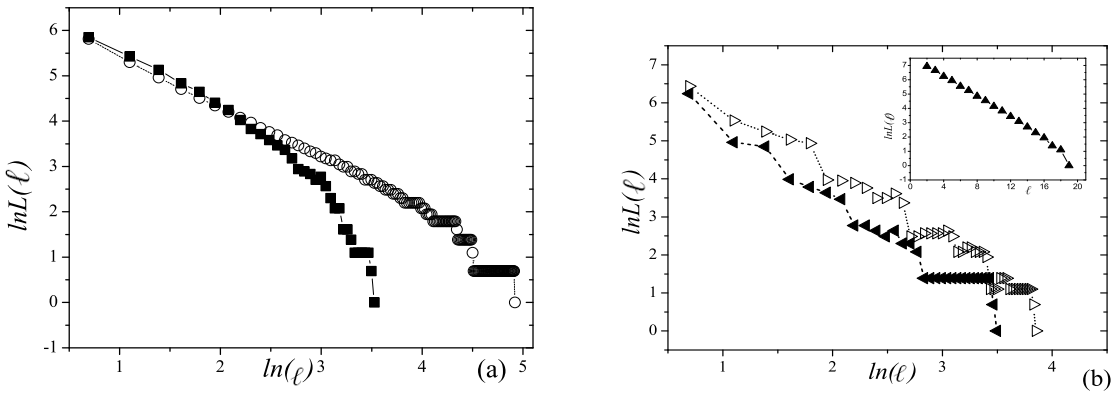

FIG. 6: Scaling regime between $L(\ell) \times \ell$. (a) Results for SW ($N = 1000, p_r = 0.01$) and ER ($N = 580, p_a = 0.002$), where scaling is quite evident. (b) In the large panel, results for DHL and WHL (with same N as in Figure 1). In the inset, results for CT (N=1534), with exponential dependence indicating infinite Euclidian and fractal dimensions.

degree is very large. Thus, oscillations set it, changing the assortative character at each step. For the WHL, very large oscillations are also observed, although they do not reach the extremal values as for DHL. Indeed, in this situation, the presence of the cross bonds lead to a large heterogeneity in the degree of the nodes, what causes a decrease in the amplitudes of oscillations.

F. Fractal dimension

As discussed in Section II, we can make use of the results obtained in the evaluation of the higher order neighborhoods to obtain the network fractal dimension d_F as proposed in . Results for the distinct networks are summarized in Figure 6. Confirming results reported in [13], it shows that, for many networks, this definition leads to a power law dependence between the quantities $L(\ell)$ and ℓ. Although our results support the definition for d_F, it also confirms that finite size effects and very short diameter raises intrinsic difficulties to its evaluation for many networks.

So, we see in Figure 6a that, for SW networks, well defined scaling region can be found for very small values of p_r, when D becomes large enough. In Figure 6b, DHL and WHL also

show scaling behavior, although the decrease of $L(\ell)$ proceeds through a series of large size steps. The slope of both curves are similar (~ 1.82), but differ from the values obtained for the usual fractal dimension [22]. We observe, in the inset of Figure 6a, that the CT definitely follows an exponential rather than power law decay. This corresponds to an infinite value for d_F, what is in agreement with the fact that it is not possible to associate a finite dimension to the tree, where the number of sites in the bulk and surface have the same order of magnitude. These results confirm that the definition of d_F is sound, capturing the essential features of quite distinct networks but, as in the case of DHL, values for d_F may differ from those obtained from other definitions.

For AN and SF networks, where the only free parameter is the number of nodes, a roughly linear alignment of points, like those in Figure 6a, is also identified, whenever over only a short range of ℓ, limited by the small values of D. For ER networks, this is also the typical behavior, unless p_a is very small, as illustrated in Figure 6a. There, a very small value of p_a warrants a fairly well defined scaling region between $L(\ell)$ and ℓ.

On closing this section, we would like to recall that the investigation of higher order neighborhoods for some well known networks opens the door to a large number of results that have not been taken into account sofar. In all subsections we were able to reproduce known results for the network indices when $\ell = 1$ and, at the same time, present some very peculiar features for the same parameters when evaluated at larger values of ℓ. In this first investigation we make the the decision to draw definite conclusions only from the most relevant situations, but we are aware that, within the large amount of information we obtained, many secondary aspects of our investigation have not been fully discussed. Nevertheless, we are sure to have shown that this framework offers, many perspectives to the understanding and characterization of the larger structures in a complex network. After exploring the $M(\ell)$'s matrices on their own, in the next section we will push forward a new investigation based on the assembly of all of them, in a single matrix $\widehat{\mathbf{M}}$. Actually, we explore the possibility of defining a quantitative measure distance between networks with the same number of nodes, based on the properties of their higher order neighborhoods.

IV. DISTANCE CONCEPTS IN NETWORK NEIGHBORHOOD SPACE

In the last Section, we developed a systematic procedure to obtain more details on the structure of networks by evaluating a set of known indices for their higher order neighborhoods. Now we want to explore the information of the neighborhood structure contained in $\widehat{\mathbf{M}}$ to another difficult challenge, namely *comparing* and *measuring* distance among networks. Addressing this task requires the attention to several issues regarding definitions and procedures, and can not be completely covered in a single step. Here, we want to tackle some aspects of this general problem, suggesting measures and methods to test whether they are particularly suitable to allow for such comparison.

Actually, this issue constitutes an extension of a classical problem within the framework of graph theory, namely, once we are given two graphs, to decide whether they are isomorphic or not. It is in fact a hard issue: the isomorphism problem for graphs is one of the non-polynomial (NP) questions, which remains still unknown whether it is NP-complete or not [23]. It has been followed mostly by mathematicians and computer scientists, who have developed several methods, algorithms and computer softwares that address this question, among these, one very fast and known is NAUTY [24], which classifies nodes according information about their immediate neighborhood; however there are also proposals [25] to improve this method considering neighbors of higher distance. A positive answer to the isomorphism question, which is very rare due to the multitude of distinct networks, completely solves the network comparison problem. However, a negative one does not advance much in providing a measure of how close the two networks (or graphs) are. The identification of all neighborhoods of a network and of the neighborhood matrix $\widehat{\mathbf{M}}$ opens perspectives for addressing the question of comparison between networks.

First let us note that, as stated before, color or gray code plots offers the possibility of visualizing the full network neighborhood structure, as exemplified in Figure 7a-d. There, we show some examples of the neighborhood plots, including in (a) that for the open end linear chain (LC) with links between nearest and next-nearest neighbors. Apart from the open end detail, LC coincides with the used SW networks with $p_a = 0$. The diameter of LC is $D = [N/2]$, resulting in a smoothly varying colors from the diagonal to the opposite matrix corners. The other three examples illustrate the situation for some other typical (ER, SW and SF) networks we investigate in this work, making it is possible to recognize,

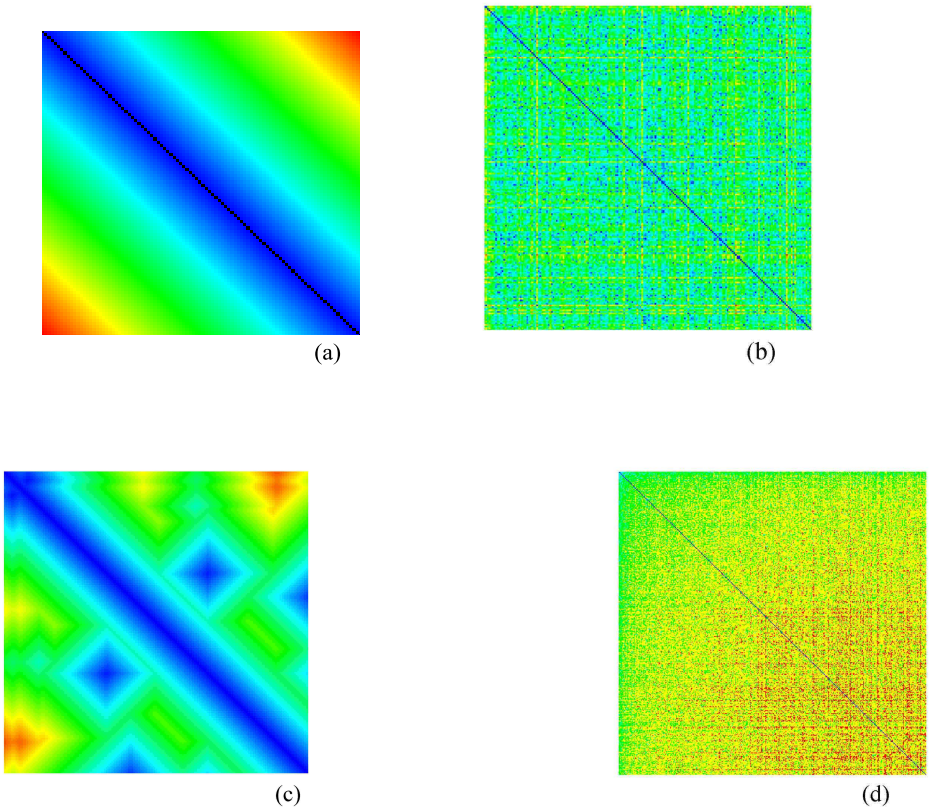

FIG. 7: Color plots of $\widehat{\mathbf{M}}$ for networks LC (a), ER (b), SW (c) and SF (d). Color runs from blue when $\ell = 1$ through red, for $\ell = D$. Number of color levels is equal to D. Values of (N,D) for (a)-(d) are given by, respectively, $(100, 50), (582, 33), (1000, 136), (1000, 6)$. In (b), $p_a = 0.002$ and in (c) $p_r = 0.01$.

respectively: b) full randomness of colors in ER network; c) the emergence of a few islands (in blue) due to the long range links added over the LC structure on the top of which SW is built; d) a color gradient towards the upper-left corner of $\widehat{\mathbf{M}}$, indicating that the low numbered sites, which have been introduced in early stages of the construction of the SF network, are at a much smaller number of steps apart from the other sites.

It is important to call the attention that the representation of a network by its color/gray plot of $\widehat{\mathbf{M}}$ depends on the particular numbering for the nodes that is being used. For the examples shown in Figure 7, the numbering follows the most natural way from the construction algorithm for the three networks, i.e., by the order in which they are introduced in the network. On the other hand, we illustrate the dependence of the color patterns on the

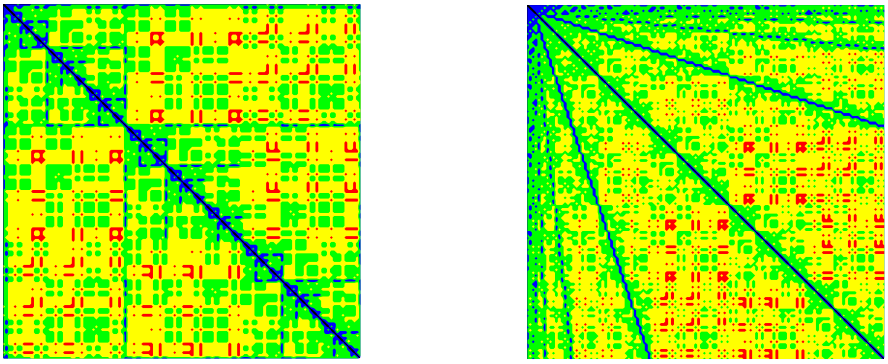

(a) (b)

FIG. 8: Color representation of the $\widehat{\mathbf{M}}$ for AN, when $N = 124$, $D = 4$, with two distinct numberings. (a) Numbering defined in [26]. (b) Starting from numbering in (a), and ordering numbers according to decreasing order of the node degree.

used numbering in Figure 8, with two images for the same AN. The first one is based on an specific numbering scheme used before [26]), while the second one results from numbering the nodes according to their decreasing degree. We notice in Figure 8b that the structure for large values of ℓ, represented by red spots, is preserved by the renumbering, but moved for the region of larger values of (i, j).

These images suggest, in a quite natural way, to compare two networks with the help of the corresponding $\widehat{\mathbf{M}}$'s, both of which, with exception of the diagonal, have only nonzero matrix elements. We restrict our comparison between networks that have exactly the same number of nodes N. Thus, the basic principle behind the methodology is to measure a *Euclidian-like distance* $\mathfrak{D}(\alpha, \beta)$, between two networks α and β, by summing over the *positive* differences between matrix elements of the two corresponding neighborhood matrices $\widehat{M_\alpha}$ and $\widehat{M_\beta}$,

$$\mathfrak{D}^2(\alpha, \beta) = \frac{1}{N(N-1)} \sum_{i,j=1}^{N} ((\widehat{M_\alpha})_{i,j} - (\widehat{M_\beta})_{i,j})^2. \tag{5}$$

Note that we consider the distance per matrix element, and that other definitions, based e.g., on the absolute values between the matrix elements, can be used within the proposed framework as well. We would like to stress that networks α and β can only be identical if they also share the same value of D and the same set of links $L(\ell), \ell = 1, ..., D$. Otherwise,

$\mathfrak{D}(\alpha,\beta)$ can never vanish. We note also that $\mathfrak{D}(\alpha,\beta)$ could hardly have the meaning of an actual distance if defined only on the basis of the information in the adjacency matrices $M_\alpha(1)$ and $M_\beta(1)$. Indeed, the fact that these are prone of zero elements would rend much less precise the results based on a similar scheme as the one we propose. In other words, $\widehat{M_\beta}$ is able to set up a much more precise measure of distance than $M(\ell=1)$.

One may ask whether it is possible to extend this procedure in order to compare networks α and β with distinct diameters $D_\alpha \neq D_\beta$. In such situation, the networks are never isomorphic, but one can also ask how far apart they are, in the sense that pairs of nodes that belong to $O_\alpha(\ell=1)$ are close to those $O_\beta(\ell=1)$, while those in $O_\alpha(\ell=D_\alpha)$ are close to those $O_\beta(\ell=D_\beta)$. Of course, pairs of nodes with intermediary values of ℓ in both networks should also come closer to one another. We find out that, to this purpose, it becomes necessary to redefine $\mathfrak{D}(\alpha,\beta)$.

Indeed, equation (5) does not properly take into account the distinct contributions in order to warrant an interpretation of distance as discussed before: pairs of sites in $O(\ell=1)$ can indeed vanish their contribution to $\mathfrak{D}(\alpha,\beta)$, but those at $O(\ell=\max(D_\alpha,D_\beta))$ will never succeed doing the same. Therefore, we introduce a new distance $\mathfrak{d}(\alpha,\beta)$ according to

$$\mathfrak{d}^2(\alpha,\beta)=\frac{1}{N(N-1)}\sum_{i,j=1}^{N}\left[\frac{(\widehat{M_\alpha})_{i,j}}{D_\alpha}-\frac{(\widehat{M_\beta})_{i,j}}{D_\beta}\right]^2. \tag{6}$$

We clearly see that, on normalizing the terms of $\mathfrak{d}(\alpha,\beta)$ to the $[0,1]$ interval, it differs from $\mathfrak{D}(\alpha,\beta)$ only by a constant factor when $D_\alpha = D_\beta$. For the more general situations $D_\alpha \neq D_\beta$, this definition avoids the large contributions coming from quite distinct values of $\widehat{M}$ to $\mathfrak{D}(\alpha,\beta)$, and accomplishes our intention to properly compare pairs of nodes in the whole ℓ interval.

If we proceed within graph theory and find that the networks α and β are isomorphic, this indicates that they are essentially the same. Thus, they differ only by the choice made for numbering the sites, but share the same topology, which depends only on the way the links are distributed among pairs of nodes. On the other hand, if we find that, for this specific choice of isomorphic networks, $\mathfrak{d}(\alpha,\beta)\neq 0$, we must conclude that their nodes are numbered differently, this result just reflecting the fact that $\widehat{\mathbf{M}}$ depends on the way the nodes are numbered. If we enumerate both networks according to one same rule, we obtain $\mathfrak{d}(\alpha,\beta)=0$

In a general situation, given two arbitrary networks, it is expected that $\mathfrak{d}(\alpha,\beta) \neq 0$. However, since $\mathfrak{d}(\alpha,\beta)$ depends on the used node numbering, it is possible to scan over the space of $N!$ distinct numberings for one of the lattices, say R_β, in order to identify, decrease or even eliminate nonzero contributions to $\mathfrak{d}(\alpha,\beta)$ stemming from the node numbering. Differences in $\mathfrak{d}(\alpha,\beta)$ resulting from distinct topologies of the networks are essential, and can not be removed by the renumbering procedure.

To accomplish this purpose, after being sure that $\mathfrak{d}(\alpha,\beta) \neq 0$, we use a Monte Carlo (MC) algorithm in order to find a better numbering for the β network, in the sense that the value of $\mathfrak{d}(\alpha,\beta)$ is reduced, while holding fixed the original numbering for the α network. In each MC step, the number of two randomly chosen sites (say s and t) of R_β are exchanged if $\mathfrak{d}'(\alpha,\beta) < \mathfrak{d}(\alpha,\beta)$, where $\mathfrak{d}'(\alpha,\beta)$ represents the new distance, evaluated by taking into account renumbering lines and columns of $\widehat{M_\beta}$ by letting $s \rightleftarrows t$. If $\mathfrak{d}'(\alpha,\beta) > \mathfrak{d}(\alpha,\beta)$, renumbering occurs with probability $\sim \exp(-(\mathfrak{d}' - \mathfrak{d})/T)$, where T is the usual Monte Carlo "temperature".

With similar results, we have also succeeded in reducing $\mathfrak{d}(\alpha,\beta)$ with a deterministic procedure. Here, we first scrutinize the terms in (6), looking for the line in matrix $\widehat{M_\beta}$ (say s) with the largest contribution to $\mathfrak{d}$. After this step, we identify the line t in $\widehat{M_\beta}$ which, moved to the position s, minimizes the value of $\mathfrak{d}$, and exchange the corresponding lines and columns $s \rightleftarrows t$. If none of the lines produces a smaller value for $\mathfrak{d}(\alpha,\beta)$ than s, we take the line with next largest contribution to $\mathfrak{d}(\alpha,\beta)$, and so on.

We use these two procedures to find (local) minima of $\mathfrak{d}^{min}(\alpha,\beta)$, which may eventually correspond to the absolute minimum. Whether this last possibility has been met can only be decided after several runs of the randomized MC algorithm, or if we succeed finding $\mathfrak{d}^{min}(\alpha,\beta) = 0$ by either of the renumbering procedures. Of course we also expect that $\mathfrak{d}^{min}(\alpha,\beta) = \mathfrak{d}^{min}(\beta,\alpha)$, but we should keep track that, in both renumbering procedures, the first network keeps the original numbering. Therefore, after performing the minimization to find $\mathfrak{d}^{min}(\alpha,\beta)$, we obtain the numbering for R_β that brings it as close as possible to that of the original numbering of R_α, the corresponding matrix of which is denoted as $\widehat{\mathbf{M}}_{\beta\to\alpha}$. Loosely speaking, it represents, in the space of all possible networks, a kind of projection of the R_β onto the direction defined by R_α. We will use this concept in the discussion of our results in the next section.

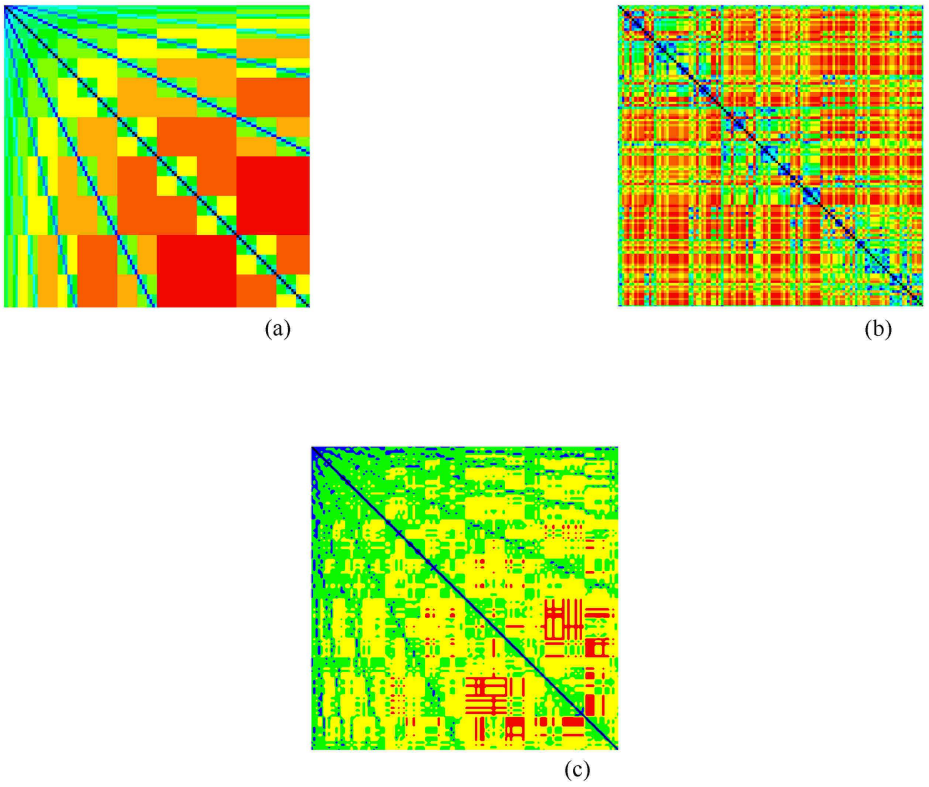

FIG. 9: Color representation of $\widehat{\mathbf{M}}$ for a number of networks. As in Figure 8, $N = 124$. In (a), (b) and (c), patterns for, respectively $\widehat{\mathbf{M}}_{CT}$, $\widehat{\mathbf{M}}_{CT\to AN}$, and $\widehat{\mathbf{M}}_{AN\to CT}$. $D_{AN} = 4$, $D_{CT} = 14$.

V. EVALUATION OF NETWORK NEIGHBORHOOD DISTANCES

In order to validate the minimization methodologies described before, we compared several pairs of identical networks. Each pair was obtained from one given $\widehat{M}_\alpha$, while $\widehat{M}_\beta$ is obtained by randomly shuffling pairs of lines and columns. This procedure ensures that both networks share the same topology, differing only by the label assigned to each node. Thus, the distance $\mathfrak{d}^{min}(\alpha, \beta)$ is expected vanish if the minimization strategies work properly. Both algorithms proved to be reliable, being able to reach $\mathfrak{d}(\alpha, \beta) = 0$ for a very large set of number-randomized network pairs.

The renumbering algorithms have then been applied to a large number of pairs of matrices α and β, for which we also generate the corresponding $\widehat{\mathbf{M}}_{\beta\to\alpha}$ and $\widehat{\mathbf{M}}_{\alpha\to\beta}$. In Figure 9(a-c) we illustrate how this scheme works in the cases of the AN and the CT: In (a), (b) and

(c) we draw, respectively, the original $\widehat{\mathbf{M}}_{CT}$, in which the nodes are numbered in concentric circles, starting from any arbitrary point, $\widehat{\mathbf{M}}_{CT\to AN}$, where the same numbering scheme in Figure 8a is used, and $\widehat{\mathbf{M}}_{AN\to CT}$.

A first comparison of Figures 8(b) and 9(a) shows that the neighborhood structures of AN and CT are indeed much more alike than one could infer by visual comparison between Figures 8(a) and 9(a). In particular, diverging rays from the upper left corner corresponding to low values of ℓ is a common feature to both networks. Further comparisons among the two figures indicate that the renumbering procedure causes a migration of the original patterns to the one of the network it is projected on. Such fine details, as changes in the angles formed by the diverging rays, are identified when we also consider Figure 9c. It shows that the angles have changed with respect to those in Figure 8b, following the values present in Figure 9a. Similar evidences from the success of the renumbering CT according to the original numbering in [26] is provided by the comparison of Figures 8a and 9b. All these effects are present despite the fact that the diameters differ considerably ($D_{AN} = 4$, $D_{CT} = 14$), the later requiring more colors/gray levels to represent each distinct value of ℓ.

These examples illustrate, in a very clear way, the discussion, in the previous Section, on the contributions to distance between networks resulting from adopted numbering and topological nature. Finally, it should be remarked that the obtained value for $\mathfrak{d}^{min}(AN, CT)$ does not depend on the initial numbering of the minimization process, apart of typical fluctuations in the MC and deterministic processes.

The values obtained for $\mathfrak{d}^{min}(\alpha, \beta)$ depends on the different kinds to which α and β belong. Besides this obvious dependence, $\mathfrak{d}^{min}$ may also depend on the number of nodes N, as well as on values assumed for some parameter defining networks, as p_a and p_r. Therefore, to render the discussion clearer, we will discuss the effect of these factors in separate.

To investigate the dependence of $\mathfrak{d}^{min}$ on network sets, we first consider the completely ordered LC, together with the AN, CT and SF networks. Four distinct samples, obtained from the same random algorithm with distinct seeds, are chosen to represent the SF network, while presented results are averages taken over the distinct samples. Initially we analyze networks that are small in size ($N = 124$), but the resulting values for $\mathfrak{d}^{min}$ are typical for networks in these sets, as we shall see later on. The results in Figure 10a represent the absolute minimum found over a series of renumbering experiments. They reveal that $\mathfrak{d}^{min}$ assumes smallest values for the (SF,SF) pair, followed by (AN,SF), (AN,CT) and (SF,CT).

As expected, LC lies at much largest distance from the other three, specially with respect to the CT. For this particular combination, $\mathfrak{d}^{min} \simeq 0.45$ reaches the largest value in the whole investigation. The entry (SF,SF) indicates the average value over the 6 possible distinct pairs that can be formed from the 4 networks. We observe that, although they are built by the same algorithm, the average distance between them is non-zero and comparable to that for the (AN,CT) pair. We notice that, while the already quoted networks quantifiers accurately express statistical similarity among members of a same network set, they are not able to uncover expressive differences among the actual neighborhood structures for distinct samples within the SF network set, as the analysis of $\mathfrak{d}$ does. On the other hand, a relative small value for $\mathfrak{d}^{min}(AN, CT)$ goes along with several other properties of AN, which are found to be quite similar to those of SF networks.

The effect of N in the values of $\mathfrak{d}^{min}$ can be checked in the same set of networks, as none of them depend on any tuning parameter. Therefore, in Figure 10b we show that the increase in the value of N to 1096 only slightly affects the previous results. The measure $\mathfrak{d}^{min}$ stays almost invariant with respect to the increase in N, and also with respect to which sample has been used to represent the SF network. This shows that $\mathfrak{d}^{min}$ is reliable in capturing the geometrical and topological differences among the distinct networks, so that it can indeed be used as a measure of their distance.

To investigate distances among networks in the same set, but with distinct values of control parameter, we consider sets of SW and ER networks. In Figures 10 (c) and (d) we show the behavior of $\mathfrak{d}^{min}$ for distinct values of p_r and p_a, holding fix the value of N.

For the purpose of a better comparison, we also include the value $p_r = 0$ into the set of investigated SW networks. The results for the largest value $p_r = 0.2$ is typical for all non-zero values of p_r. It assumes minimal values along the diagonal, i.e. when $p_{r,\alpha} = p_{r,\beta}$ and increases when one moves away from it, enlarging the difference between $p_{r,\alpha}$ and $p_{r,\beta}$. The overall feature of (10c) is that of a valley along the main diagonal. In a quantitative way, typical values in the diagonal are given by $\mathfrak{d}^{min} \sim 0.14$, what is somewhat smaller than that obtained for the SF ($\mathfrak{d}^{min} \sim 0.15$) shown in (10a) and (10b). The maximal value $\mathfrak{d}^{min}$ in the investigated range of p_r is 0.27 for $\mathfrak{d}^{min}(p_r = 0, p_r = 0.2)$. Note that this value is some 20% larger than that found for $\mathfrak{d}^{min}(SF, CT)$. Therefore, we see that pairs of networks grown according to different rules can produce smaller values of $\mathfrak{d}^{min}$ than pairs of networks originated by the same procedure, whenever distinct values of one or more control

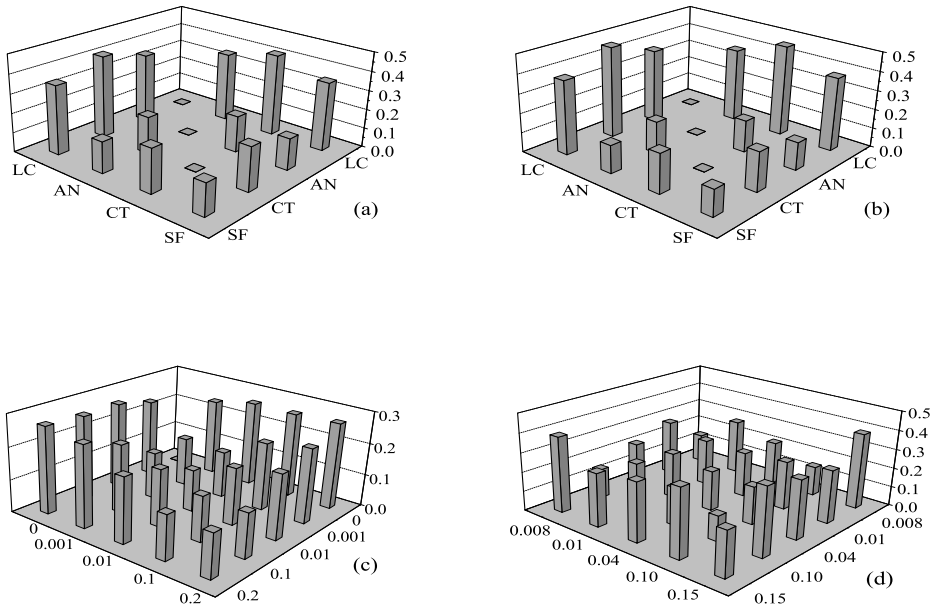

FIG. 10: Representation of $\mathfrak{d}^{min}$ by 3D bars (vertical axis) for distinct situations. (a) $N = 124$, and four distinct networks, as indicated in the x and y axis labels. (b) The same networks, but for $N = 1096$. (c) and (d) Axis labels indicate five distinct values of p_r and p_a, used in the analysis of the SW and ER network sets, with $N = 1000$.

parameters, which one might guess to be more alike.

Finally, the results in Figure 10d for the ER set, where the range of values for p_a is similar to that used for p_r, goes in other direction in comparison to SW. It is difficult to recognize a clear pattern, reinforce the random character of this network class. Values for $\mathfrak{d}^{min}$ along the diagonal are also among the smallest, but near diagonal pairs can also show similar distances. If we fix to the largest value of α, and let β vary, no monotonic behavior is found as before. From the quantitative point of view, the mean value along the diagonal $\simeq 0.19$ is higher than those for SW or SF. The maximal off-diagonal value $\simeq 0.39$ is more than 30% higher that the corresponding value for the SW set.

VI. CONCLUSIONS

In this work we put forward, in a systematic way, the investigation of the higher order neighborhoods of a complex network R. The basic concepts, that have been introduced in a previous work, are developed in many aspects, opening new paths for the exploration of properties related to structures in a larger scale than that of the immediate vicinity of a node. According to the basic idea, each neighborhood $O(\ell)$, represented by an adjacency matrix $M(\ell)$, is regarded as a network in itself, so that many distinct quantifiers used for network characterization can be used to obtain the properties of each neighborhood.

The large amount of results we obtain can be casted into two parts. The first one encompasses all results obtained from each $M(\ell)$, while the second is related to properties of $\widehat{\mathbf{M}}$, which condenses, in a single matrix, all information on the neighborhood structure.

In the discussion of the distinct quantifiers, we find that many of them behave in a oscillatory way with respect to ℓ. This is the case of $C(\ell)$ for self-similar networks, as CT, DHL, WHL, as well as for hypercubic lattices. For ER and SW networks, oscillatory behavior in $C(\ell)$ can also be found, provided linking and rewiring probabilities are small enough. Interesting enough, the values of $\langle k(\ell)\rangle$ oscillate for both DHL and WHL, for all ℓ range. For all other networks, the average node degree $\langle k(\ell)\rangle$ increases exponentially for several networks, but this behavior can be masked, for networks with very small values of D. Hierarchical property and scale-free distribution of nodes are rare events for large values of ℓ. Nevertheless, we present examples of SF, AN and WHL, where corresponding power law distributions for $p(k;\ell)$ and $C(k;\ell)$ are found for $\ell > 1$. Properties related to degree assortativity or dissortativity are likely to remain the same as ℓ increases. One exception, again due to the emergence of oscillatory behavior, refers to the self similar DHL and WHL. Finally, we use the information obtained from the set $M(\ell)$ to evaluate the fractal dimension of all investigated networks. The obtained results reproduce well into the expected values, among which we quote $d_F \to \infty$ for CT, smaller values of d_F for less connected networks, and some troubles in finding precise values when the network diameter is very small.

The properties of $\widehat{\mathbf{M}}$ can be used for a variety of purposes. The simple visualization of $\widehat{\mathbf{M}}$ with the help of color codes can be very helpful for identifying and understanding the large scale structure of networks. Such procedure naturally evolves to the question of finding which representation, depending on the node numbering adopted, is more suitable to be used

for a given network. Examples for the deterministic AN illustrate how distinct they can be. Furthermore, since a minimization Monte-Carlo algorithm finds the best way a given network can be *projected* onto a second one, we address the issue of defining and evaluating the distance between networks based on the neighborhood structure contained in $\widehat{\mathbf{M}}$. We present results that support, in quantitative and qualitative way, the usefulness of this framework. We can assign quantitative values for a distance function, which corresponds to several intuitive notion of distinct structures, as that between LC and CT. The results we obtain also reveal that, despite the fact that the members of a set of networks, generated by the same algorithm, share the same values of the usual network indices, their actual neighborhood structure can remain very distant from each other, specially for the ER situation.

This series of investigations we open in this work is very large and can be explored in many directions. They certainly include a finer exploration of sets of well known networks as well as analyzes of data from actual networks. Efforts to extract further information along new lines from the matrices $M(\ell)$ and $\widehat{\mathbf{M}}$ are on consideration as well.

Acknowledgement: This work was partially supported by CNPq and FAPESB.

---

[1] J. L. Gross, and J. Yellen *Handbook of Graph Theory*, Discrete Mathematics and its Applications, (CRC Press Boca Raton 2000).

[2] S. N. Dorogovtsev and J. F. F. Mendes, *Evolution of Networks: From Biological Nets to the Internet and WWW*, (Oxford Univ. Press, 2003).

[3] S. Boccaletti, V. Latora, Y. Moreno, M. Chavez, and D. -U Hwang, Phys. Rep. **424**, 175 (2006).

[4] M. E. J. Newman, A.-L. Barabási, and D. J. Watts, *The Structure and Dynamics of Networks*, (Princeton University Press, 2006)

[5] M. E. J. Newman, SIAM Review **45**, 167 (2003).

[6] R. Albert, and A.-L. Barabási, Rev. Mod. Phys **74**, 47 (2002).

[7] M. E. J. Newman, Phys. Rev. Lett. **89**, 208701 (2002).

[8] A. Fronczak, J. A. Holyst, M. Jedynak, and J.Sienkiewicz, Physica A **316**, 688 (2002).

[9] L. F. Costa, Phys. Rev. Lett. **93** 098702 (2004).

[10] R. Xulvi-Brunet, and J. M. Sokolov, Acta Physica Polonica B **36**, 1431 (2005).

[11] G. Caldarelli, R. Pastor-Santorras and A. Vespignani, Eur. Phys. J. B **38**, 183-186 (2004).

[12] R. F. S. Andrade, J. G. V. Miranda, and T. P. Lobao, Phys. Rev. E **73**, 046101 (2006).

[13] C. Song, S. Havlin, H. A. Makse, Nature **433**, 392 (2005).

[14] D. J. Watts and S.H. Strogatz, Nature **393**, 440 (1998).

[15] A.-L. Barabási, and R. Albert, Science **286**, 509 (1999).

[16] P. Erdös, and A. Rényi, Publ. Math. (Debrecen), **6**, 290 (1959).

[17] J.S. Andrade Jr., H.J. Herrmann, R.F.S. Andrade, and L.R. daSilva, Phys. Rev. Lett. **94**, 018702 (2005).

[18] M. Kaufman, and R. B. Griffiths, Phys. Rev. B **26**, 5282 (1982).

[19] E. Ravasz, and A-L Barabási, Phys. Rev. R **67**, 026112 (2003).

[20] J. E. Whitesitt, *Boolean Algebra and its Applications*, (Dover, New York, 1995).

[21] F. Harary, *Graph Theory*, (Perseus Books Publishing, Cambridge 1995).

[22] J. R. Melrose, J. Phys. A: Math.Gen. **16**, 3077 (1983).

[23] J. Torán, SIAM J. Comput. **33**, 1093 (2004).

[24] B. McKay, Congressus Numerantium, **30**, 45 (1981).

[25] T. Miyazaki, DIMACS Ser. Discrete Math. Theoret. Comput. Sci., **28**, 239 (1997).

[26] R.F.S. Andrade, and J.G.V. Miranda, Physica A **356**, 1 (2005).